Decrease in intramuscular lipid droplets and translocation of HSL in response to muscle contraction and epinephrine

Clara Prats,[1],* Morten Donsmark,* Klaus Qvortrup,[†] Constantine Londos,[§] Carole Sztalryd,** Cecilia Holm,[††] Henrik Galbo,[§§] and Thorkil Ploug*

Copenhagen Muscle Research Center, Department of Medical Physiology,* Panum Institute, University of Copenhagen, DK-2200 Copenhagen N, Denmark; Department of Medical Anatomy,[†] Panum Institute, University of Copenhagen, DK-2200 Copenhagen N, Denmark; Laboratory of Cellular and Developmental Biology,[§] National Institute of Diabetes and Digestive and Kidney Diseases, National Institutes of Health, Bethesda, MD 20892-8028; Geriatric Research, Education, and Clinical Center,** Baltimore Veterans Affairs Health Care Center, Department of Medicine, School of Medicine, University of Maryland, Baltimore, MD 21201; Department of Experimental Medical Science,[††] University of Lund, BMC C11, SE-221 84, Lund, Sweden; and Copenhagen Muscle Research Center, Department of Rheumatology,[§§] Bispebjerg Hospital, DK-2400 Copenhagen NV, Denmark

Abstract A better understanding of skeletal muscle lipid metabolism is needed to identify the molecular mechanisms relating intramuscular triglyceride (IMTG) to muscle metabolism and insulin sensitivity. An increasing number of proteins have been reported to be associated with intracellular triglyceride (TG), among them the PAT family members: perilipin, ADRP (for adipocyte differentiation-related protein), and TIP47 (for tail-interacting protein of 47 kDa). Hormone-sensitive lipase (HSL) is thought to be the major enzyme responsible for IMTG hydrolysis in skeletal muscle. In adipocytes, regulation of HSL by intracellular redistribution has been demonstrated. The existence of such regulatory mechanisms in skeletal muscle has long been hypothesized but has never been demonstrated. The aim of this study was to characterize the PAT family proteins associated with IMTG and to investigate the effect of epinephrine stimulation or muscle contraction on skeletal muscle TG content and HSL intracellular distribution. Rat soleus muscles were either incubated with epinephrine or electrically stimulated for 15 min. Single muscle fibers were used for morphological analysis by confocal and transmission electron microscopy. We show a decrease in IMTG in response to both lipolytic stimuli. Furthermore, we identify two PAT family proteins, ADRP and TIP47, associated with IMTG. Finally, we demonstrate HSL translocation to IMTG and ADRP after stimulation with epinephrine or contraction.—Prats, C., M. Donsmark, K. Qvortrup, C. Londos, C. Sztalryd, C. Holm, H. Galbo, and T. Ploug. **Decrease in intramuscular lipid droplets and translocation of HSL in response to muscle contraction and epinephrine.** *J. Lipid Res.* 2006. 47: 2392–2399.

Supplementary key words lipid metabolism regulation • skeletal muscle • hormone-sensitive lipase • adipocyte differentiation-related protein • tail-interacting protein of 47 kDa

Interest in skeletal muscle lipid metabolism has increased exponentially during the last decades. One of the reasons is the repeatedly reported inverse relation between intramuscular triglyceride (IMTG) concentrations and insulin sensitivity (1–5). Paradoxically, endurance training is well known to increase insulin sensitivity, whereas it has been shown to increase IMTG content (6, 7). Thus, it seems that IMTG content may not directly determine insulin sensitivity. A better understanding of skeletal muscle lipid metabolism is required to identify the molecular mechanisms involved in the effect of IMTG content on muscle metabolism and insulin sensitivity.

For many years, it has been debated whether IMTGs are used during exercise, but today this question remains unresolved. The most likely explanation for the discrepancy between previous studies is that, in most of them, chemical methods to measure triglyceride (TG) were used. Such methods cannot distinguish between IMTG and TG contained in adipocytes surrounding muscle fibers. Illustrating the problem, Donsmark et al. (8) showed that the TG content of a single adipocyte ($\sim$0.3 nmol) corresponds to $\sim$5% of the TG content of a 2 mg soleus muscle sample, but the adipocyte volume makes up only 0.01% of the sample. Therefore, decreases in IMTG may have been undetected, being masked by contaminating TG from adipocytes (9).

IMTG is stored within intracellular lipid droplets (LDs). LDs were initially considered to be relatively static

Abbreviations: ADRP, adipocyte differentiation-related protein; HSL, hormone-sensitive lipase; IMTG, intramuscular triglyceride; LD, lipid droplet; PKA, cyclic AMP-dependent protein kinase; TEM, transmission electron microscopy; TG, triglyceride; TIP47, tail-interacting protein of 47 kDa.

[1] To whom correspondence should be addressed.
   e-mail: cprats@mfi.ku.dk

This article is available online at http://www.jlr.org

structures in which lipids were stored. However, during the last decade, it has become increasingly clear that LDs are much more dynamic and complexly regulated than originally thought. The core of LDs is composed of cholesteryl esters and TGs, whereas the surface has been shown to be a phospholipid monolayer of unique fatty acid composition (10). The interface between the LDs and the cytoplasm contains a complex network of filaments and tubular structures (11, 12). An increasing number of proteins have been reported to associate with LDs, most notably the members of the PAT family: perilipin, adipocyte differentiation-related protein (ADRP or adiphophilin), and tail-interacting protein of 47 kDa (TIP47). Perilipin is detected exclusively surrounding LDs in adipocytes and steroidogenic cells (13, 14). Both ADRP and TIP47 show sequence similarity to perilipin, but unlike perilipin, ADRP is expressed ubiquitously, whereas TIP47 is expressed in some nonadipose cells (15).

Hormone-sensitive lipase (HSL) (EC 3.1.1.3) has long been accepted as the lipolysis rate-limiting enzyme in adipocytes (16, 17). HSL was detected for the first time in rat skeletal muscle several years ago (18). However, growing evidence in the literature suggests the existence of one or more neutral lipases, other than HSL, with considerable activity in skeletal muscle (for review, see ref. 19). In the nonstimulated state, HSL has 10-fold higher activity toward diacylglycerol than toward TG (20). Moreover, lipolysis in HSL-knockout mice causes diacylglycerol accumulation in adipose tissue, muscle, and testis (21). These and other observations suggest that HSL may be responsible for diacylglycerol hydrolysis, more than being involved in the initial TG hydrolysis. Recently, a novel TG lipase was discovered and named adipose triglyceride lipase. Adipose triglyceride lipase is expressed predominantly in white and brown adipose tissue, with progressively decreasing expression in testis, cardiac muscle, and skeletal muscle (22). Considering the different substrate specificities of adipose triglyceride lipase and HSL, it has been suggested that the hydrolysis of the first ester bond in TG is catalyzed predominantly by adipose triglyceride lipase. The resulting diacylglycerol would be hydrolyzed in turn by HSL, and the final hydrolysis of the resulting monoacylglycerol would be done by monoglyceride lipase (23). Nevertheless, HSL seems to be the rate-limiting enzyme in exercise- or epinephrine-induced lypolysis. Both epinephrine and muscle contraction have been demonstrated to increase neutral lipase activity in rat skeletal muscle homogenate, and such activation is blocked when the homogenate is incubated with an antibody against HSL before activity measurements (18, 24). Similarly, in human skeletal muscle, total neutral lipase activation has consistently been reported during exercise (25, 26), and later, it was ascribed to HSL (27). Thus, it appears reasonable to assume that HSL is the exercise-induced lipolysis rate-limiting enzyme. HSL activity is regulated by reversible phosphorylation and by allosteric mechanisms (for review, see ref. 19).

A lack of correlation between HSL activation measured chemically in vitro and lipolysis rates has been reported frequently. This may be explained by HSL intracellular redistribution, targeting HSL to the substrate in response to lipolytic stimuli, a regulatory mechanism that cannot be detected in vitro because of disruption of cellular integrity. In adipocytes, translocation of HSL to LDs has been demonstrated in response to lipolytic stimuli (28, 29). In fat cells lacking perilipin, HSL is unable to translocate to LDs in response to increased cyclic AMP levels (30). In addition, mutation of the N-terminal cyclic AMP-dependent protein kinase (PKA) sites of perilipin abolishes PKA-induced lipolysis (31, 32). This evidence has led to the hypothesis that perilipin forms a barrier around LDs and that phosphorylation of perilipin by PKA may induce a conformational change providing HSL access to TG.

The importance of HSL intracellular distribution and perilipin in the regulation of lipid metabolism in adipocytes is well established. The question arises whether, in nonadipose cells, which do not express perilipin, HSL translocates to LDs, and if so, which PAT family members could be involved. Here, we studied skeletal muscle at rest and after stimulation with epinephrine or muscle contraction to quantify IMTG and analyzed the intracellular distribution of ADRP, TIP47, and HSL by confocal microscopy.

EXPERIMENTAL PROCEDURES

Animal procedures

All experiments were approved by the Animal Experiments Inspectorate of the Danish Ministry of Justice. Male Wistar rats (∼70 g; Charles River Laboratories, Sulzfeld, Germany) were anesthetized by intraperitoneal injection of sodium pentobarbital (5 mg/100 g body weight; Pharmacy of Rigshospitalet, Copenhagen, Denmark). The aorta was cannulated and the hindquarters were perfused for 1 min (20 ml/min) with Krebs-Henseleit buffer gassed with 95% O_2 and 5% CO_2 and containing 8 mM glucose, 1 mM pyruvate, and 0.2% BSA (pH 7.4). Soleus muscles, including intact tendons, were gently dissected free and preincubated for 60 min with the perfusion medium and then continuously gassed with 95% O_2 and 5% CO_2 at 29°C. The setup for the presented experiments is described in detail elsewhere (33). After preincubation, muscles either remained resting as controls or were stimulated for 15 min with either 5.5 μM epinephrine (Pharmacy of Rigshospitalet) (18) or by electrical stimulation to perform repeated maximal tetanic contractions (200 ms series of 100 Hz, impulse duration 0.2 ms, delivered every 1 s at 25 V) (24). After incubation or treatment, muscles were fixed and single fibers teased as described previously (34).

Morphological quantification of IMTG. The classical biochemical method to determine muscle TG has been criticized for having a large coefficient of variation, attributable to the contamination of muscle biopsies with adipocytes or remnants of adipocytes. Here, we used a morphological determination of IMTG, by staining single muscle fibers with Bodipy-493/503 (Invitrogen) and subsequent analysis by confocal microscopy. Single muscle fibers were transferred to PBS and incubated for 30 min with Bodipy-493/503 (2 μg/ml in PBS). After three washes with PBS for 10 min each, muscle fibers were mounted in Vectashield (Vector Laboratories, Burlingame, CA) on a glass slide and analyzed by confocal microscopy.

Immunofluorescence study in single muscle fibers. Immunostaining of single muscle fibers was performed as described previously (34). The primary antibodies used were a rabbit anti-HSL antibody raised and affinity-purified against recombinant rat HSL (35), an anti-ADRP produced in goat against the murine N-terminal peptide (amino acids 1–28), and a rabbit anti-TIP47 produced against the murine C-terminal fragment (amino acids 191–437) of the peptide crystallized previously (36). Secondary antibodies were conjugated to either Alexa-568 or Alexa-488 (Invitrogen). For costaining of LDs, Bodipy-493/503 was added to the secondary antibody solution (2 μg/ml).

Confocal microscopy imaging and quantification. Confocal images were collected on a TCS SP2 microscope (Leica) as described previously (34). Confocal images were collected from the surface and from 6 μm deep inside the muscle fibers, each being 0.3 μm apart in the z-plane. From each muscle, a minimum of six single muscle fibers were analyzed, and from each fiber, imaging was performed in three randomized areas. From each area, four planes were used in each position, surface and inside the muscle fiber, to obtain average and maximal projections, which were used for quantification and visualization, respectively. Images were analyzed using Metamorph software (Universal Imaging Corp.).
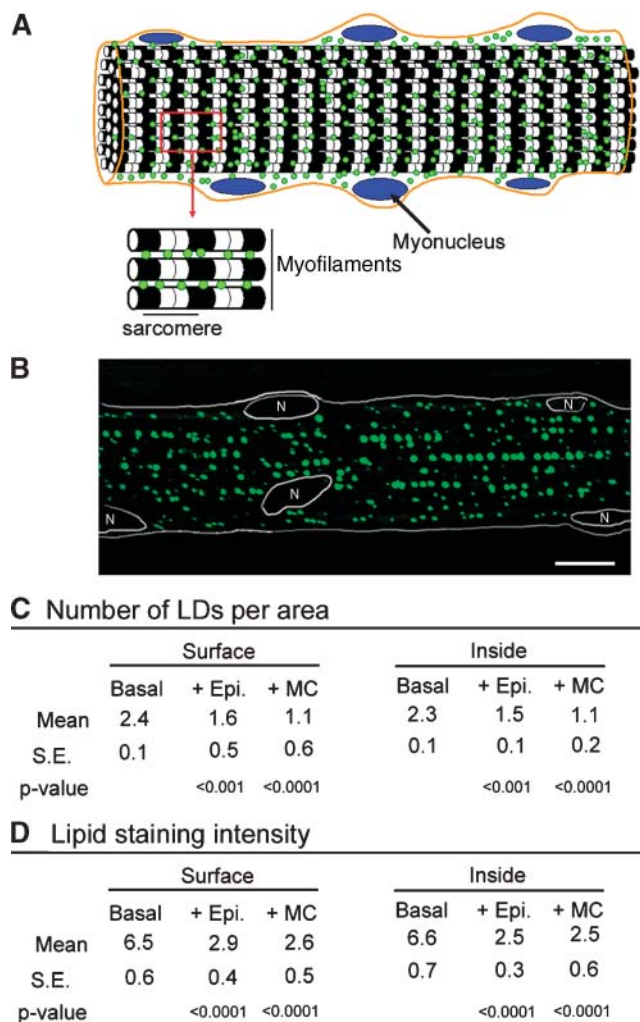
Transmission electron microscopy study in single muscle fibers. Single muscle fibers were immunostained for transmission electron microscopy (TEM) as described previously (34). The primary antibody against HSL described above was used. Secondary antibody was conjugated to a 1.4 nm gold cluster (Nanoprobes, Inc.), and silver enhancement was performed (HQ Silver; Nanoprobes, Inc.). Samples were examined in a Philips CM 100 transmission electron microscope operated at an accelerating voltage of 80 kV. Images were collected using a SIS Megaview II digital camera and Analysis software.

Statistical analyses. Quantification was performed on three randomized areas within a single muscle fiber. The obtained value per analyzed area was used to calculate a mean value per muscle fiber. From each muscle biopsy, a minimum of six single muscle fibers were analyzed, and the mean value from each of them was used to obtain a mean value per muscle biopsy. All data are presented as means ± SEM of five independent experiments. Statistical significance was assessed by Mann-Whitney test and is represented as follows: * $P < 0.05$, ** $P < 0.01$, *** $P < 0.005$.

RESULTS

IMTG content decreases in response to epinephrine and muscle contraction

IMTG was stained with Bodipy-493/503 in rat soleus single muscle fibers. A cartoon of a single muscle fiber is shown in **Fig. 1A**. Confocal microscopy imaging was performed at the surface and at a depth of 6 μm inside fibers. In Fig. 1B, a representative maximal projection of four confocal images taken at the surface of a muscle fiber is shown. Quantification of the number of LDs per area was performed (Fig. 1C). At the surface, in the cytosol underneath the plasma membrane, the number of LDs decreased significantly by 33% and 54% in response to epinephrine and muscle contraction, respectively. Similarly, the number of LDs inside, at the cytosol between

C Number of LDs per area

	Surface			Inside		
	Basal	+ Epi.	+ MC	Basal	+ Epi.	+ MC
Mean	2.4	1.6	1.1	2.3	1.5	1.1
S.E.	0.1	0.5	0.6	0.1	0.1	0.2
p-value		<0.001	<0.0001		<0.001	<0.0001

D Lipid staining intensity

	Surface			Inside		
	Basal	+ Epi.	+ MC	Basal	+ Epi.	+ MC
Mean	6.5	2.9	2.6	6.6	2.5	2.5
S.E.	0.6	0.4	0.5	0.7	0.3	0.6
p-value		<0.0001	<0.0001		<0.0001	<0.0001

Fig. 1. Intramuscular triglyceride (IMTG) content decreases in response to epinephrine and muscle contraction. Muscle fibers are polynuclear cells with a dense and compact core of myofilaments, where the contractile apparatus is found organized as repeated sarcomeres. Myonucleus (N) are distributed at the periphery of the fibers. A: Schematic cartoon showing the intracellular distribution of lipid droplets (LDs) (green) in the cytosol underneath the plasma membrane and between myofilaments of a single muscle fiber. LDs were stained with Bodipy-493/503 in single muscle fibers from rat soleus muscle. Confocal microscopic imaging was performed in the cytoplasm beneath the plasma membrane and in the cytoplasm between the myofilaments (6 μm deep from the surface). B: Representative image of the intracellular distribution of LDs at the surface of a muscle fiber (bar = 10 μm). C, D: Results are expressed as number of LDs per area (number of detected lipid profiles in 135 μm^2) (C) and as intensity of lipid staining (total gray value per pixel) (D). Basal, epinephrine-stimulated (+Epi.), and contracted (+MC) muscle fibers were analyzed. Note the significant decreases in both the number of LDs per area and the intensity of lipid staining in response to epinephrine and muscle contraction at the surface as well as inside muscle fibers. Results are expressed as means ± SEM of five independent experiments, from each of which a minimum of six fibers were analyzed.

myofilaments, decreased by 35% and 52% after epinephrine incubation and muscle contraction, respectively. The intensity of lipid staining per area was taken as a measure of IMTG content. In parallel with the decrease in the num-

ber of LDs, a significant decrease in lipid staining in response to both lipolytic stimuli was detected (Fig. 1D). In basal fibers, the intensity of lipid staining at the surface and inside was similar. After epinephrine stimulation, lipid content decreased significantly by 55% and 62% underneath the sarcolemma and inside muscle fibers, respectively. A similar decrease was detected after 15 min of muscle contraction, with 60% and 62% decreases at the surface and inside muscle fibers, respectively. Furthermore, we measured the average size of the LDs in basal and stimulated muscles. In agreement with the finding that the lipid content decreased relatively more than the number of LDs, the average size of the LDs at the surface of muscle fibers decreased by 28% ($P < 0.05$) and 29% ($P < 0.01$) in response to epinephrine and muscle contraction, respectively. Inside muscle fibers, similar 29% ($P < 0.01$) and 38% ($P < 0.005$) decreases were detected in response to epinephrine and muscle contraction, respectively.

ADRP and TIP47 are associated with intramuscular LDs

Single muscle fibers were stained with Bodipy-493/503 and immunostained for either ADRP or TIP47. LDs are different from other intracellular organelles in that their surface is covered by a phospholipid monolayer and their core is packed with lipid esters. This makes the choice of fixation and permeabilization important to preserve LDs as well as their associated proteins. Here, we used formaldehyde fixation followed by permeabilization by saponin, which has been shown to be appropriate for the visualization of LDs and associated proteins (37). Nevertheless, we could not exclude the possibility that some LDs may have been washed out by saponin during the immunostaining protocol. Therefore, we quantified the number of LDs after immunostaining and compared these results with the results presented above, in which staining of LDs was performed in the absence of saponin. After incubation with saponin, the number of LDs decreased 43% at the surface and 25% inside muscle fibers, compared with staining in the absence of saponin. The intracellular distribution of ADRP and TIP47 was studied with respect to the remaining LDs, and representative images are shown (**Fig. 2**). Note that ADRP was associated mainly with the LDs, whereas TIP47 was associated with LDs as well as forming small cytosolic clusters. To study the dynamics of the ADRP and TIP47 association with LDs in response to epinephrine and muscle contraction, the percentage of lipid surface colocalizing with ADRP or TIP47 was quantified. No significant changes in the percentage of the LD surface colocalizing with ADRP in response to epinephrine or muscle contraction were detected, being 86 ± 3% in basal conditions, 86 ± 2% in epinephrine-stimulated muscle fibers, and 80 ± 2% after in vitro muscle contraction ($P > 0.05$). Furthermore, when the percentage of the LD surface that colocalized with TIP47 was quantified, we detected no significant differences among the three groups of muscles. In basal muscle fibers, 76 ± 3% of LD surface colocalized with TIP47 signal, whereas after epinephrine stimulation and muscle contraction, the per-
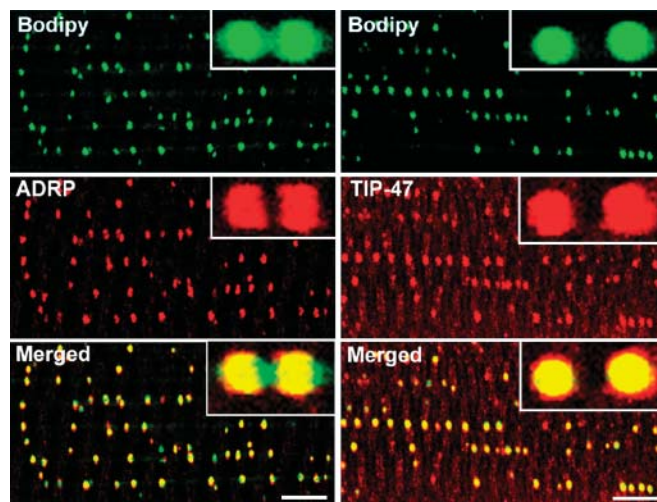

Fig. 2. Adipocyte differentiation-related protein (ADRP) and tail-interacting protein of 47 kDa (TIP47) are associated with intramuscular LDs. A: Single muscle fibers were immunostained for ADRP or TIP47, whereas LDs were stained with Bodipy-493/503 (green). A secondary antibody conjugated to Alexa-568 (red) was used to detect ADRP and TIP47 primary antibodies. Representative images of the intracellular distributions of TIP47, ADRP, and LDs are shown. In the lower panel, merged images are shown in which colocalization between both proteins and LDs can be seen in yellow (bars = 2.5 μm). Note that both ADRP and TIP47 are associated with LDs in skeletal muscle. Higher magnification images of ADRP and TIP47 associated with two intramuscular LDs are shown in the top right corner of each panel. These images are representative of five independent experiments, from each of which a minimum of six fibers were analyzed.

centages were 81 ± 4% and 76 ± 3%, respectively ($P > 0.05$). Coimmunostaining of ADRP and TIP47 was performed, and quantification of the percentage of ADRP that colocalized with TIP47 showed no significant differences in response to epinephrine incubation or muscle contraction. At the surface, 44 ± 4% of ADRP colocalized with TIP47 in basal fibers, and after epinephrine incubation or muscle contraction, the percentage was 53 ± 3% or 42 ± 4%, respectively ($P > 0.05$). Inside muscle fibers, the percentages of colocalization between ADRP and TIP47 were 52 ± 3% in basal conditions, 46 ± 3% after epinephrine incubation, and 44 ± 3% after muscle contraction ($P > 0.05$). Thus, our results suggest a constant proportion between ADRP and TIP47 associated with a certain amount of neutral lipids, which does not differ between the LDs at the surface or inside muscle fibers or in response to either lipolytic stimulus.

HSL intracellular redistribution in response to epinephrine and muscle contraction

To study HSL intracellular distribution, LDs were stained with Bodipy-493/503 and immunostaining of HSL was performed. Representative images of LD and HSL intracellular distribution are shown (**Fig. 3A**). In basal muscle fibers, HSL was found at the cytoplasm, showing a dotted pattern distributed throughout the muscle fibers and being more condensed at the myofibrillar cross-striations with a periodicity corresponding to that of sarcomeres. In
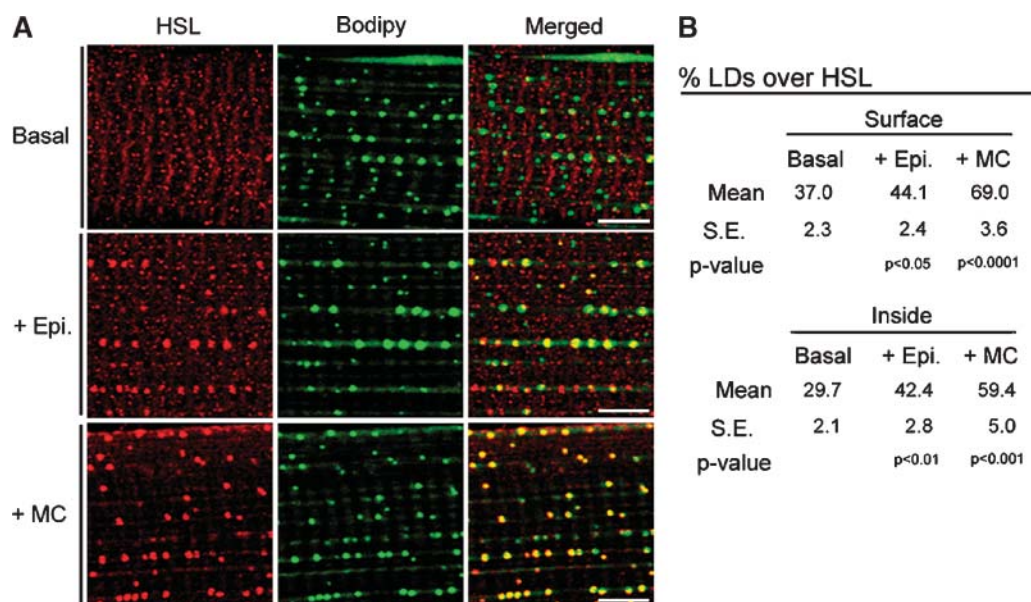
Fig. 3. Hormone-sensitive lipase (HSL) intracellular redistribution to LDs in response to epinephrine and muscle contraction. Intramuscular LDs were stained with Bodipy-493/503 (green), and immuno-staining of HSL was performed and detected with a secondary antibody conjugated to Alexa-568 (red). A: Representative images of LDs stained with Bodipy-493/503 and HSL intracellular distribution in basal, epinephrine-stimulated (+Epi.), and contracted (+MC) muscles are shown. In the right panels, merged images are presented in which an increase in the colocalization between LDs and HSL in response to both lipolytic stimuli can be seen in yellow (bars = 2.5 μm). B: The percentage of LDs stained with Bodipy-493/503 that colocalized with HSL was quantified in basal, epinephrine-stimulated, and contracted muscle fibers. Note the significant increases in the percentage of colocalization between LDs and HSL at the surface (top table) and inside muscle fibers (bottom table). Results are expressed as means ± SEM of five independent experiments. From each muscle, a minimum of six fibers were analyzed.
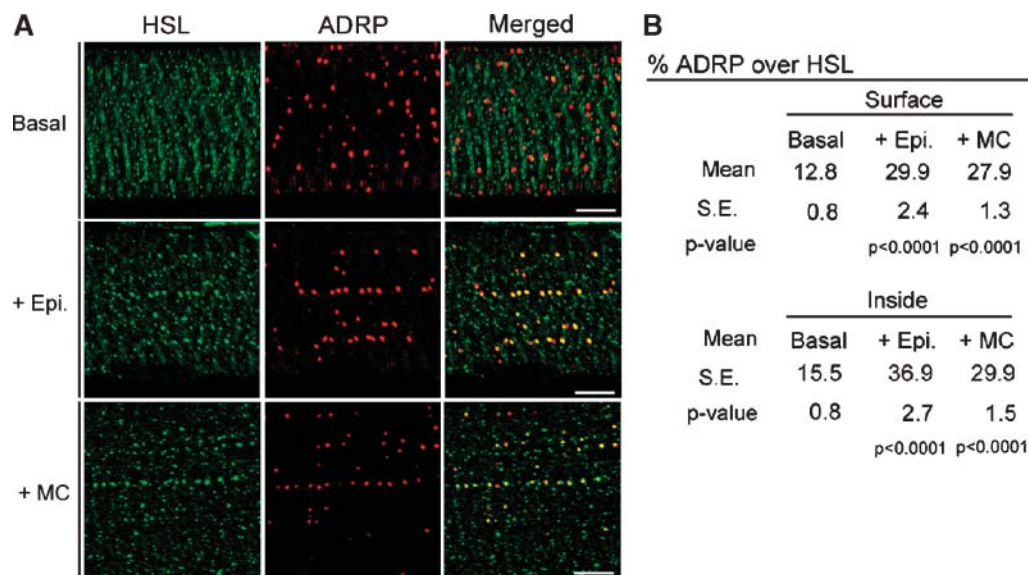
response to epinephrine and muscle contraction, an increase in the colocalization between LDs and HSL can be seen (Fig. 3A, right panels). In response to both epinephrine and muscle contraction, a decrease in HSL, found as small dots and at the cross-striations, coincided with an increase in HSL associated with LDs. Quantification of LD and HSL colocalization was performed (Fig. 3B). At muscle fiber surfaces, the percentage of the LD surface that colocalized with HSL increased significantly from 37% in basal muscle to 44% and 69% in response to epinephrine and muscle contraction, respectively. Moreover, a similar increase was detected inside muscle fibers, where the percentage of colocalization increased from 30% in basal fibers to 42% and 59% after stimulation with epinephrine and muscle contraction, respectively. Here, we present the first evidence of HSL translocation to LDs in skeletal muscle in response to epinephrine or muscle contraction.

Because ADRP has been accepted as an LD marker (15), coimmunostaining of HSL and ADRP was performed to confirm the HSL translocation to LDs detected by Bodipy-493/503 staining. In **Fig. 4A**, representative images of HSL and ADRP intracellular distribution are shown. Quantification of the percentage of ADRP that overlapped with HSL showed a significant increase in response to both stimuli at the surface and inside muscle fibers (Fig. 4B).

At the surface of muscle fibers, 13% of ADRP colocalized with HSL in basal muscle fibers. After epinephrine stimulation or muscle contraction, the percentage increased to 30% or 28%, respectively. A similar response was detected inside muscle fibers, where colocalization between ADRP and HSL increased from 15% in basal conditions to 37% or 30% after epinephrine stimulation or muscle contraction, respectively. These results confirm that in response to both lipolytic stimuli, HSL translocates to LDs.

Study of HSL intracellular distribution by TEM

Single muscle fibers were immunostained for HSL for TEM to confirm the HSL translocation to intramuscular LDs reported above. The immunoreaction is seen as black electron-dense deposits, because gold particles conjugated with the secondary antibodies were silver-enhanced. In both basal and stimulated muscle fibers, a variable fraction of HSL was associated with LDs and the remainder was found in the cytoplasm as small clusters (**Fig. 5A**, arrows). Representative images of an LD in basal soleus muscle with nearly no associated HSL are shown in Fig. 5B, C. After either epinephrine stimulation or muscle contraction, an increase in HSL associated with LDs was detected, and representative images of an LD with increased amounts of associated HSL can be seen in Fig. 5D, E. These results

A HSL ADRP Merged

B % ADRP over HSL

	Surface		
	Basal	+ Epi.	+ MC
Mean	12.8	29.9	27.9
S.E.	0.8	2.4	1.3
p-value		p<0.0001	p<0.0001

	Inside		
	Basal	+ Epi.	+ MC
Mean	15.5	36.9	29.9
S.E.	0.8	2.7	1.5
p-value		p<0.0001	p<0.0001

Fig. 4. HSL intracellular redistribution to ADRP in response to epinephrine and muscle contraction. Coimmunostaining of ADRP and HSL was performed in single muscle fibers. To detect ADRP and HSL, secondary antibodies conjugated to Alexa-568 (red) and Alexa-488 (green) were used, respectively. A: Representative images of ADRP and HSL intracellular distribution in basal, epinephrine-stimulated (+Epi.), and contracted (+MC) muscle fibers are shown. In the right panels, colocalization between both proteins can be seen in yellow (bars = 2.5 μm). B: Quantification of the percentage of ADRP that colocalized with HSL was performed at the surface and inside single fibers from basal, epinephrine-stimulated, and contracted muscle. Note the significant increases in the percentage of colocalization between ADRP and HSL at the surface (top table) and inside muscle fibers (bottom table). Results are expressed as means ± SEM of five independent experiments. From each muscle, a minimum of six fibers were analyzed.

confirm HSL translocation to the LDs in response to both lipolytic stimuli.

DISCUSSION

The major findings of this study are that in vitro stimulation of rat soleus muscle with either epinephrine or muscle contraction induces a decrease in IMTG. Furthermore, ADRP and TIP47 are associated with intramuscular LDs, and HSL translocates to the LDs in response to both lipolytic stimuli.

Because this is the first study in which the intracellular distribution of LDs has been analyzed in single muscle fibers, it is important to note that no differences in the number of LDs per area or in lipid content were found between the cytoplasm beneath the sarcolemma and the cytoplasm between myofilaments. Thus, in rat soleus muscle, LDs are homogeneously distributed throughout muscle fibers. Furthermore, LDs found at these two regions had a similar proportion of associated ADRP and TIP47, and they responded similarly to epinephrine and muscle contraction.

Although for many years it has been debated whether IMTGs are used during exercise, this remains unresolved because of conflicting results on the variation of IMTG content in response to exercise reported in previous studies. Such controversy could be explained by limitations in the methodology used to measure TG. The biochemical method classically used cannot distinguish between IMTG and TG contained in adipocytes surrounding muscle fibers. Therefore, decreases in IMTG may have been undetected, being masked by contaminating TG from adipocytes. However, considering that potential variations in IMTG content reflect the net balance between TG breakdown (lipolysis) and synthesis from FFAs (38), another possible explanation for the controversy could be that, in lipolytic states, increases in lipolysis rates could be accompanied by increases in IMTG synthesis rates, resulting in no net IMTG decrease. Accordingly, to reveal true intramuscular lipolysis, we developed a morphological method to quantify IMTGs in single muscle fibers and incubated muscle in the absence of FFAs to abolish TG synthesis. Using confocal microscopy, IMTGs stained with Bodipy-493/503 were easily distinguished from extramyocellular TGs. Here, we show a significant decrease in IMTG in response to a rather brief stimulation with epinephrine or muscle contraction. Such a decrease was detected as reductions in the number of LDs (Fig. 1C), in the intensity of neutral lipid staining (Fig. 1D), and in the average size of the LDs.

Increasing evidence in the literature indicates that the PAT proteins have a fundamental role in lipid metabolism. In fully differentiated skeletal muscle, we present proof of the association of two PAT family members, TIP47 and ADRP, with LDs (Fig. 2). Morphological analysis of ADRP and TIP47 intracellular distribution show that ADRP is associated mainly with LDs, whereas TIP47 is associated
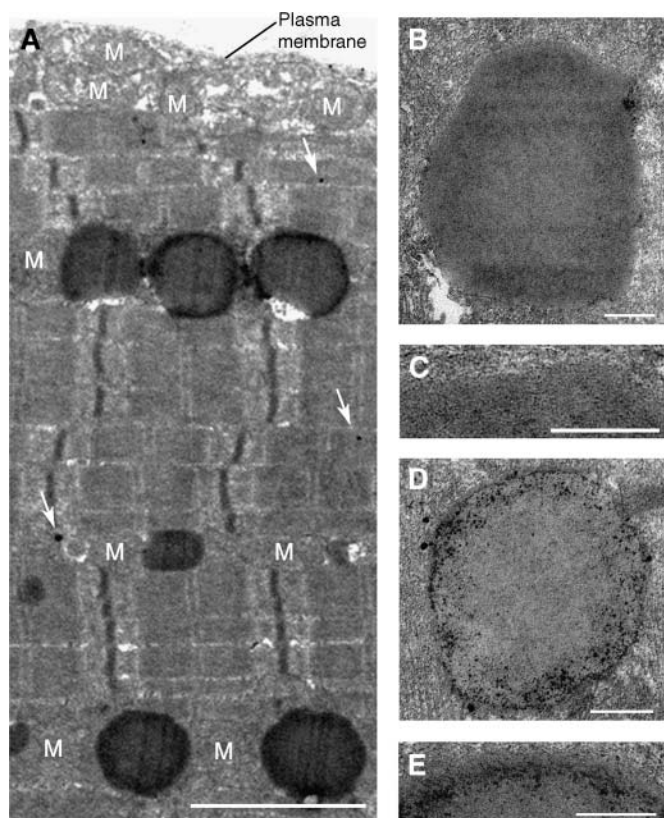
Fig. 5. Study of HSL intracellular distribution by transmission electron microscopy (TEM). Single muscle fibers from basal and stimulated muscle were used for immunostaining against HSL. Secondary antibody conjugated to nanogold particles was used, followed by silver enhancement. Representative TEM images of HSL intracellular distribution are shown. Immunoreaction is seen as black electron-dense precipitate. A: Skeletal muscle HSL can be found at the cytosol as small clusters (arrows) or associated with LDs. Note that LDs are always found surrounded by mitochondria (M) (bar = 3 μm). B–E: Higher magnification TEM images of intramuscular LDs give proof of HSL translocation to LDs. Note the increases in the amount of HSL associated with the surface of LDs from basal (B, C) to stimulated (D, E) muscle fibers (bars = 200 nm).

with LDs as well as in small cytosolic clusters. A similar intracellular distribution of TIP47 has been reported in other cell types (39, 40). The importance of perilipin in the regulation of lipid metabolism in adipocytes seems clear. However, little is known about the role of ADRP and TIP47 as the PAT proteins coating LDs in nonadipose cells (for review, see ref. 38). Recently, in CHO cells, it was shown that ADRP is ubiquitinated and degraded by proteolysis when TG levels decreased and that inhibition of ADRP proteolysis led to a 2.8-fold increase in TG levels (41). Furthermore, improvement of human skeletal muscle insulin sensitivity is related to the upregulation of ADRP levels (42), and the downregulation of ADRP and TIP47, using small interfering RNA treatment in AML-12 murine liver cells, perturbs lipid metabolism and insulin signaling (C. Sztalryd, unpublished observations). Such data suggest that, like perilipin, ADRP and TIP47 could protect LD contents from lipases and may protect cells from poten-

tial effects of fatty acids on insulin action and from the development of insulin resistance. On the other hand, the fact that TIP47 has been shown to be associated with LDs (39) and with the endosomal trafficking system (40) has led to speculations about different potential cellular functions. In HeLa cells grown in standard low-lipid-containing culture medium, a significant portion of TIP47 has been shown to move from the cytosolic fraction to the LD fraction after lipid loading of the medium, whereas the distribution of ADRP did not change (39), suggesting that TIP47 may be involved in neutral lipid intracellular trafficking. In any case, these potential roles of ADRP and TIP47 imply a dynamic association and dissociation of both proteins to and from the LDs. Our results show no significant changes in the percentage of ADRP or TIP47 colocalizing with LDs in response to either epinephrine or contraction, a fact that, considering the detected decrease in the number and size of LDs after both stimuli, indicates a dynamic dissociation of both PAT proteins from the hydrolyzed LDs.

Intracellular redistribution of HSL to the LDs in response to lipolytic stimuli has been demonstrated to be an important regulatory mechanism of lipid metabolism in adipocytes (28, 29). The existence of such a regulatory mechanism in skeletal muscle has long been hypothesized but has never been demonstrated. We show that in both basal and stimulated muscle fibers, a fraction of HSL was found at the cytoplasm, showing a dotted pattern of distribution throughout the muscle fibers (Figs. 3, 4). In response to epinephrine or muscle contraction, HSL translocated to LDs (Fig. 3), which are coated with ADRP (Fig. 4). Moreover, HSL translocation to LDs is further supported by TEM images showing HSL at the surface of LDs (Fig. 5). In fat cells lacking perilipin, HSL is unable to translocate to LDs (30). Whether ADRP and/or TIP47 are involved in the regulation of HSL binding to LDs in skeletal muscle remains to be elucidated. Nevertheless, in adipocytes of perilipin-null mice, a compensatory increase of ADRP has been reported, whereas in fibroblasts of ADRP-null mice, a compensatory increase of TIP47 expression has been shown (38), suggesting that ADRP and/or TIP47 in nonadipose cells could play a similar role to that of perilipin in adipocytes, regulating HSL binding to LDs.

Further studies are needed to elucidate the regulatory mechanisms of HSL intracellular distribution and to understand the roles played by ADRP and TIP47 in skeletal muscle.

REFERENCES

1. Jacob, S., J. Machann, K. Rett, K. Brechtel, A. Volk, W. Renn, E. Maerker, S. Matthaei, F. Schick, C. Claussen, et al. 1999. Association of increased intramyocellular lipid content with insulin resistance in lean nondiabetic offspring of type 2 diabetic subjects. *Diabetes.* **48:** 1113–1119.

2. Perseghin, G., P. Scifo, F. De Cobelli, E. Pagliato, A. Battezzati, C. Arcelloni, A. Vanzulli, G. Testolin, G. Pozza, A. Del Maschio, et al. 1999. Intramyocellular triglyceride content is a determinant of in vivo insulin resistance in humans: a ^{1}H-^{13}C nuclear magnetic resonance spectroscopy assessment in offspring of type 2 diabetic parents. *Diabetes.* **48:** 1600–1606.

3. Krssak, M., K. F. Petersen, A. Dresner, L. DiPietro, S. Vogel, D. Rothman, M. Roden, and G. Shulman. 1999. Intramyocellular lipid concentrations are correlated with insulin sensitivity in humans: a ^{1}H NMR spectroscopy study. *Diabetologia.* **42:** 113–116.

4. Pan, D., S. Lillioja, A. Kriketos, M. Milner, L. Baur, C. Bogardus, A. Jenkins, and L. Storlien. 1997. Skeletal muscle triglyceride levels are inversely related to insulin action. *Diabetes.* **46:** 983–988.

5. Goodpaster, B., R. Theriault, S. Watkins, and D. Kelley. 2000. Intramuscular lipid content is increased in obesity and decreased by weight loss. *Metabolism.* **49:** 467–472.

6. Decombaz, J., B. Schmitt, M. Ith, B. Decarli, P. Diem, R. Kreis, H. Hoppeler, and C. Boesch. 2001. Postexercise fat intake repletes intramyocellular lipids but no faster in trained than sedentary subjects. *Am. J. Physiol. Regul. Integr. Comp. Physiol.* **281:** R760–R769.

7. Goodpaster, B., J. He, S. Watkins, and D. Kelley. 2001. Skeletal muscle lipid content and insulin resistance: evidence for a paradox in endurance-trained athletes. *J. Clin. Endocrinol. Metab.* **86:** 5755–5761.

8. Donsmark, M., J. Langfort, C. Holm, T. Ploug, and H. Galbo. 2005. Hormone-sensitive lipase as mediator of lipolysis in contracting skeletal muscle. *Exerc. Sport Sci. Rev.* **33:** 127–133.

9. Wendling, P., S. Peters, G. Heigenhauser, and L. Spriet. 1996. Variability of triacylglycerol content in human skeletal muscle biopsy samples. *J. Appl. Physiol.* **81:** 1150–1155.

10. Tauchi-Sato, K., S. Ozeki, T. Houjou, R. Taguchi, and T. Fujimoto. 2002. The surface of lipid droplets is a phospholipid monolayer with a unique fatty acid composition. *J. Biol. Chem.* **277:** 44507–44512.

11. Franke, W. W., M. Hergt, and C. Grund. 1987. Rearrangement of the vimentin cytoskeleton during adipose conversion: formation of an intermediate filament cage around lipid globules. *Cell.* **49:** 131–141.

12. Novikoff, A. B., P. M. Novikoff, O. M. Rosen, and C. S. Rubin. 1980. Organelle relationships in cultured 3T3-L1 preadipocytes. *J. Cell Biol.* **87:** 180–196.

13. Greenberg, A. S., J. J. Egan, S. A. Wek, N. B. Garty, E. J. Blanchette-Mackie, and C. Londos. 1991. Perilipin, a major hormonally regulated adipocyte-specific phosphoprotein associated with the periphery of lipid storage droplets. *J. Biol. Chem.* **266:** 11341–11346.

14. Servetnick, D., D. L. Brasaemle, J. Gruia-Gray, A. R. Kimmel, J. Wolff, and C. Londos. 1995. Perilipins are associated with cholesteryl ester droplets in steroidogenic adrenal cortical and Leydig cells. *J. Biol. Chem.* **270:** 16970–16973.

15. Londos, C., D. L. Brasaemle, C. J. Schultz, J. P. Segrest, and A. R. Kimmel. 1999. Perilipins, ADRP, and other proteins that associate with intracellular neutral lipid droplets in animal cells. *Semin. Cell Dev. Biol.* **10:** 51–58.

16. Holm, C., T. G. Kirchgessner, K. L. Svenson, G. Fredrikson, S. Nilsson, C. G. Miller, J. E. Shively, C. Heinzmann, R. S. Sparkes, T. Mohandas, et al. 1988. Hormone-sensitive lipase: sequence, expression, and chromosomal localization to 19 cent-q13.3. *Science.* **241:** 1503–1506.

17. Fredrikson, G., P. Stralfors, N. Nilsson, and P. Belfrage. 1981. Hormone-sensitive lipase of rat adipose tissue. Purification and some properties. *J. Biol. Chem.* **256:** 6311–6320.

18. Langfort, J., T. Ploug, J. Ihlemann, M. Saldo, C. Holm, and H. Galbo. 1999. Expression of hormone sensitive lipase and its regulation by adrenaline in skeletal muscle. *Biochem. J.* **340:** 459–465.

19. Kiens, B. 2006. Skeletal muscle lipid metabolism in exercise and insulin resistance. *Physiol. Rev.* **86:** 205–243.

20. Straalfors, P., H. Olsson, and P. Belfrage. 1987. Hormone-Sensitive Lipase. *In* The Enzymes. 18th edition. P. D. Boyer and E. G. Krebs, editors. Academic Press, New York. 147–177.

21. Haemmerle, G., R. Zimmermann, M. Hayn, C. Theussl, G. Waeg, E. Wagner, W. Sattler, T. Magin, E. Wagner, and R. Zechner. 2002. Hormone-sensitive lipase deficiency in mice causes diglyceride accumulation in adipose tissue, muscle, and testis. *J. Biol. Chem.* **277:** 4806–4815.

22. Zimmermann, R., J. Strauss, G. Haemmerle, G. Schoiswohl, R. Birner-Gruenberger, M. Riederer, A. Lass, G. Neuberger, F. Eisenhaber, A. Hermetter, et al. 2004. Fat mobilization in adipose tissue is promoted by adipose triglyceride lipase. *Science.* **306:** 1383–1386.

23. Zechner, R., J. Strauss, G. Haemmerle, A. Lass, and R. Zimmermann. 2005. Lipolysis: pathway under construction. *Curr. Opin. Lipidol.* **16:** 333–340.

24. Langfort, J., T. Ploug, J. Ihlemann, C. Holm, and H. Galbo. 2000. Stimulation of hormone-sensitive lipase activity by contractions in rat skeletal muscle. *Biochem. J.* **351:** 207–214.

25. Watt, M., G. Heigenhauser, M. O'Neill, and L. Spriet. 2003. Hormone-sensitive lipase activity and fatty acyl-CoA content in human skeletal muscle during prolonged exercise. *J. Appl. Physiol.* **95:** 314–321.

26. Kjaer, M., K. Howlett, J. Langfort, T. Zimmerman-Belsing, J. Lorentsen, J. Bulow, J. Ihlemann, U. Feldt-Rasmussen, and H. Galbo. 2000. Adrenaline and glycogenolysis in skeletal muscle during exercise: a study in adrenalectomised humans. *J. Physiol.* **528:** 371–378.

27. Roepstorff, C., B. Vistisen, M. Donsmark, N. Nielsen, H. Galbo, K. Green, D. Hardie, J. Wojtaszewski, E. Richter, and B. Kiens. 2004. Regulation of hormone sensitive lipase activity and Ser^{565} and Ser^{565} phosphorylation in human skeletal muscle during exercise. *J. Physiol.* **560:** 551–562.

28. Egan, J. J., A. S. Greenberg, M. K. Chang, S. A. Wek, M. C. Moos, Jr., and C. Londos. 1992. Mechanism of hormone-stimulated lipolysis in adipocytes: translocation of hormone-sensitive lipase to the lipid storage droplet. *Proc. Natl. Acad. Sci. USA.* **89:** 8537–8541.

29. Hirsch, A. H., and O. M. Rosen. 1984. Lipolytic stimulation modulates the subcellular distribution of hormone-sensitive lipase in 3T3-L1 cells. *J. Lipid Res.* **25:** 665–677.

30. Sztalryd, C., G. Xu, H. Dorward, J. T. Tansey, J. A. Contreras, A. R. Kimmel, and C. Londos. 2003. Perilipin A is essential for the translocation of hormone-sensitive lipase during lipolytic activation. *J. Cell Biol.* **161:** 1093–1103.

31. Souza, S. C., K. Muliro, L. Liscum, P. Lien, M. Yamamoto, and J. Schaffer. 2002. Modulation of hormone-sensitive lipase and protein kinase A-mediated lipolysis by perilipin A in an adenoviral reconstituted system. *J. Biol. Chem.* **277:** 8267–8272.

32. Tansey, J. T., K. Vogt, J. Davis, K. Jones, D. Fraser, D. L. Brasaemle, A. R. Kimmel, and C. Londos. 2003. Functional studies on native and mutated forms of perilipins: a role in protein kinase A-activated lipolysis of triacylglycerols. *J. Biol. Chem.* **278:** 8401–8406.

33. Langfort, J., T. Ploug, J. Ihlemann, E. Baranczuk, M. Donsmark, J. Gorski, and H. Galbo. 2003. Additivity of adrenaline and contractions on hormone-sensitive lipase, but not on glycogen phosphorylase, in rat muscle. *Acta Physiol. Scand.* **178:** 51–60.

34. Ploug, T., B. Van Deurs, H. Ai, S. W. Cushman, and E. Ralston. 1998. Analysis of GLUT4 distribution in whole skeletal muscle fibers: identification of distinct storage compartments that are recruited by insulin and muscle contraction. *J. Cell Biol.* **142:** 1429–1446.

35. Osterlund, T., B. Danielsson, E. Degerman, J. A. Contreras, G. Edgren, R. Davis, M. Schotz, and C. Holm. 1996. Domain-structure analysis of recombinant rat hormone-sensitive lipase. *Biochem. J.* **319:** 411–420.

36. Hickenbottom, S. J., A. R. Kimmel, C. Londos, and J. H. Hurley. 2004. Structure of a lipid droplet protein: the PAT family member TIP47. *Structure.* **12:** 1199–1207.

37. Ohsaki, Y., T. Maeda, and T. Fujimoto. 2005. Fixation and permeabilization protocol is critical for the immunolabeling of lipid droplet proteins. *Histochem. Cell Biol.* **124:** 445–452.

38. Londos, C., C. Sztalryd, J. T. Tansey, and A. R. Kimmel. 2005. Role of PAT proteins in lipid metabolism. *Biochimie.* **87:** 45–49.

39. Wolins, N. E., B. Rubin, and D. L. Brasaemle. 2001. TIP47 associates with lipid droplets. *J. Biol. Chem.* **276:** 5101–5108.

40. Diaz, E., and S. R. Pfeffer. 1998. TIP47: A cargo selection device for mannose 6-phosphate receptor trafficking. *Cell.* **93:** 433–443.

41. Xu, G., C. Sztalryd, X. Lu, J. T. Tansey, J. Gan, H. Dorward, A. R. Kimmel, and C. Londos. 2005. Post-translational regulation of adipose differentiation-related protein by ubiquitin/proteasome pathway. *J. Biol. Chem.* **280:** 42841–42847.

42. Phillips, S., C. Choe, T. Ciaraldi, A. Greenberg, A. Kong, S. Baxi, L. Christiansen, S. Mudaliar, and R. Henry. 2005. Adipocyte differentiation-related protein in human skeletal muscle: relationship to insulin sensitivity. *Obes. Res.* **13:** 1321–1329.